

This is the accepted manuscript made available via CHORUS. The article has been published as:

Spectral-gap analysis for efficient tunneling in quantum adiabatic optimization

Lucas T. Brady and Wim van Dam

Phys. Rev. A **94**, 032309 — Published 9 September 2016

DOI: [10.1103/PhysRevA.94.032309](https://doi.org/10.1103/PhysRevA.94.032309)

Spectral Gap Analysis for Efficient Tunneling in Quantum Adiabatic Optimization

Lucas T. Brady

Department of Physics, University of California, Santa Barbara, CA 93106-5110, USA

Wim van Dam

*Department of Computer Science, Department of Physics,
University of California, Santa Barbara, CA 93106-5110, USA*

(Dated: August 17, 2016)

We investigate the efficiency of Quantum Adiabatic Optimization when overcoming potential barriers to get from a local to a global minimum. Specifically we look at n qubit systems with symmetric cost functions $f : \{0, 1\}^n \rightarrow \mathbb{R}$ where the ground state must tunnel through a potential barrier of width n^α and height n^β . By the quantum adiabatic theorem the time delay sufficient to ensure tunneling grows quadratically with the inverse spectral gap during this tunneling process. We analyze barrier sizes with $1/2 \leq \alpha + \beta$ and $\alpha < 1/2$ and show that the minimum gap scales polynomially as $n^{1/2-\alpha-\beta}$ when $2\alpha + \beta \leq 1$ and exponentially as $n^{-\beta/2} \exp(-Cn^{(2\alpha+\beta-1)/2})$ when $1 < 2\alpha + \beta$. Our proof uses elementary techniques and confirms and extends an unpublished folklore result by Goldstone from 2002, which used large spin and instanton methods. Parts of our result also refine recent results by Kong and Crosson and Jiang et al. about the exponential gap scaling.

I. INTRODUCTION

Quantum Annealing seeks to solve optimization problems by taking a state of a quantum system and evolving its Hamiltonian to get a desired result. Quantum Adiabatic Optimization (QAO) [1] is a form of quantum annealing that seeks to keep a system in the ground state while adiabatically evolving the Hamiltonian. Quantum annealing is often compared with classical simulated annealing, which seeks the ground state of a system through temperature variation, and with simulated quantum annealing, which is a classical simulation of quantum annealing using path-integral Quantum Monte Carlo. A lot of recent work has gone into analyzing QAO in its own right [2–4] and comparing QAO with classical algorithms such as simulated quantum annealing [5–14] to see how much speed-up QAO can give if any.

It has been conjectured that a large part of QAO’s power comes from the ability of quantum systems to tunnel through potential barriers. In this article, we focus on an n -qubit Hamiltonian, but by making it symmetric in the qubits, we can effectively reduce our problem to a one-dimensional tunneling problem. This setup of one-dimensional tunneling in n symmetric qubits has been studied before by Farhi, Goldstone, and Gutmann [2] who considered tunneling through a constant width spike of height n and who showed for this setting a gap scaling of $g_{\min} \propto n^{-1/2}$. In [2], the authors also showed that QAO has an exponential speed-up over classical simulated annealing for the spike tunneling problem. This exponential speed-up over classical simulated annealing for the spike problem was one of the original impetuses for studying barrier tunneling in QAO.

Reichardt [3] showed that QAO can tunnel in constant time ($g_{\min} \propto 1$) provided that the area (width \times height) of the barrier is bounded by $\mathcal{O}(\sqrt{n})$. More recently, Crosson and Deng [8] examined thin barriers of varying height, and Kong and Crosson [15] found that sufficiently large barriers lead to exponential run-times. Jiang et al. [14] showed that Quantum Monte Carlo (QMC) can reproduce the exponential run-time

behavior of thermally assisted quantum tunneling through such large barriers. Crosson and Harrow [13] have shown that QMC can efficiently solve barrier tunneling problems for spike barriers and barriers of the size considered by Reichardt’s proof. Independently the current authors have numerically found [11] that the transitions between constant, polynomial, and exponential run-time scaling for QMC simulations coincide with the same transitions for QAO.

In this article, we consider barriers with width proportional to n^α and height proportional to n^β and mainly focus on barriers with $1/2 \leq \alpha + \beta$, which is above Reichardt’s [3] constant scaling region, and $2\alpha + \beta < 1$ which is below Kong and Crosson’s [15] exponential scaling region. We show that barriers in this intermediate size regime lead to polynomial scaling of the minimum spectral gap with $g_{\min} \propto n^{1/2-\alpha-\beta}$. Through the quantum adiabatic theorem this scaling implies that a polynomial running time is sufficient for the QAO algorithm to tunnel through such barriers. Additionally, our method also confirms Kong and Crosson’s exponential scaling and provides an exact form for the polynomial prefactor on the exponential.

In Section II, we present our problem and discuss the Hamiltonian governing the interactions of our n -qubit system. Section III presents details of previous work on this problem and highlight both the polynomial scaling region between $1/2 \leq \alpha + \beta$ and $2\alpha + \beta < 1$ where few solid results have been published and the unexplored region for $\alpha > \beta$.

Our problem lends itself to a large spin analysis using either spin coherent states [18] or the Villain transformation [19]. Section IV briefly touches on spin coherent states, which have been used to analyze this problem before [15], and presents an in depth analysis using the Villain transformation, resulting in a semi-classical Hamiltonian that describes our dynamics for large n .

Focusing on just the critical region of the problem where the spectral gap is smallest, Section V derives a model that approximates the semi-classical Hamiltonian in the large n limit. We provide several arguments for why this model accurately

represents the asymptotic behavior of our original problem. Finally, in Section VI, we use this model to derive an exact asymptotic expression for the scaling behavior of the spectral gap.

Appendix A provides an in depth look at a modified version of the Villain transformation, which we use to transform the barrier tunneling problem into a semi-classical differential equation. Our detailed analysis keeps track of the exact assumptions made and provides the scaling behavior of the next leading order terms that are ignored. This precision and robustness is in contrast with standard path-integral methods whose errors are difficult to check. The modified Villain transformation and our subsequent approximations also provide polynomial accuracy in the spectral gap, unlike spin-coherent state methods or the WKB approximation.

II. QUANTUM ADIABATIC OPTIMIZATION OF SYMMETRIC FUNCTIONS

Our main goal is to explore quantum tunneling through a barrier in a symmetric cost function $f : \{0, 1\}^n \rightarrow \mathbb{R}$ defined on the n -dimensional hypercube $\{0, 1\}^n$. Our specific cost function is

$$f(x) = |x| + b(|x|), \quad (1)$$

where $|x|$ is the Hamming Weight of the length n bit string x . The barrier function, $b : \{0, \dots, n\} \rightarrow \mathbb{R}$, is some function that is localized around $|x| = n/4$ and has width proportional to n^α and height proportional to n^β . We describe these barriers using the notation $n^\alpha \times n^\beta$.

To create an algorithm to minimize the cost function, we first encode it into a quantum Hamiltonian on n qubits:

$$H_1 = \sum_{x \in \{0, 1\}^n} f(x) |x\rangle\langle x|. \quad (2)$$

QAO starts the system in a different Hamiltonian with known and easily prepared ground state; the typical starting Hamiltonian applies a magnetic field in the \hat{x} direction so that

$$H_0 = \sum_{i=1}^n (H_0)_i \quad \text{with} \quad H_0 = \frac{1}{2} \begin{pmatrix} 1 & -1 \\ -1 & 1 \end{pmatrix}. \quad (3)$$

The ground state of H_0 is an equal superposition of all states $|x\rangle$, which corresponds to a binomial distribution in Hamming weight. Then, QAO finds the ground state of H_1 by slowly evolving the system from H_0 into H_1 using

$$H(s) = (1-s)H_0 + sH_1, \quad (4)$$

and the quantum adiabatic theorem says that the system will stay in the ground state if $0 \leq s \leq 1$ varies slowly enough. In order to ensure adiabaticity the evolution time, T , must scale depending on both the norm of $dH(s)/ds$ and the inverse of the minimum spectral gap between the two smallest eigenvalues $\lambda_1(s)$ and $\lambda_0(s)$ of $H(s)$:

$$g_{\min} := \min_{s \in [0, 1]} (\lambda_1(s) - \lambda_0(s)). \quad (5)$$

Historically, sources [1] have claimed that the adiabatic theorem requires

$$T \gg \frac{\max_s \left\| \frac{dH}{ds} \right\|}{g_{\min}^2}. \quad (6)$$

Recent work [20] has shown that the adiabatic condition may be a more complicated function of these parameters, but all of this recent work has the running time scaling like a polynomial in $1/g_{\min}$ and n . Since the norm of the Hamiltonian's derivative is usually independent of parameters such as our α and β , typically the gap is taken as the important part of this expression. Therefore, the key issue of this paper is the calculation of g_{\min} .

The Hamiltonian, $H(s)$, on n qubits can be simplified by considering just the symmetric subspace. For each Hamming weight $0 \leq h \leq n$, the Hamiltonian is degenerate on the subspace of $\{|x\rangle : |x| = h\}$, so there will only be one degenerate energy level for each Hamming Weight h . This symmetry can be utilized to rewrite the full $2^n \times 2^n$ Hamiltonian as an $(n+1) \times (n+1)$ symmetric Hamiltonian:

$$\begin{aligned} H_{\text{sym}}(s) = & \sum_{h=0}^n \left[\frac{(1-s)}{2} n + s(h + b(h)) \right] |h\rangle\langle h| \\ & - \frac{(1-s)}{2} \sum_{h=0}^{n-1} \sqrt{(h+1)(n-h)} |h\rangle\langle h+1| \\ & - \frac{(1-s)}{2} \sum_{h=0}^{n-1} \sqrt{(h+1)(n-h)} |h+1\rangle\langle h| \end{aligned} \quad (7)$$

When $b(z) = 0$, the ground state of the symmetric Hamiltonian is explicitly

$$\begin{aligned} |GS_{b(z)=0}\rangle = & \frac{1}{(2\delta(\delta+s))^{n/2}} \\ & \times \sum_{h=0}^n \sqrt{\binom{n}{h}} (s+\delta)^{n-h} (1-s)^h |h\rangle, \end{aligned} \quad (8)$$

where $\delta := \sqrt{1-2s+2s^2}$ is the unperturbed spectral gap. This distribution is a binomial for $s = 0$, and the width remains proportional to \sqrt{n} for $0 \leq s < 1$. The maximum amplitude $|h\rangle$ state here corresponds with the zero amplitude state in the first excited state and can be thought of as the center of the distribution. The center coincides with $h = \frac{n}{4}$ when $s = s^* := \frac{1}{2}(\sqrt{3}-1)$.

In the large n limit with a non-zero barrier, $b(z)$ becomes extremely narrow relative to the dimension of the Hilbert space, so for most s values, the energy states are unaffected by the barrier. It is only when the energy states get close to the barrier that the perturbation becomes important. Therefore, in the large n limit, the location of the minimum spectral gap becomes this critical s^* .

III. PREVIOUS ASYMPTOTIC RESULTS

A 2002 folklore result by Goldstone [16] says that for $\alpha < \beta$ and $\alpha < 1/2$ the minimum gap for tunneling through an

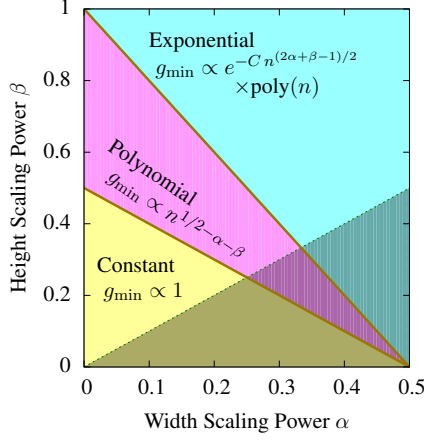


FIG. 1: The spectral gap scaling of QAO according to the original folklore result by Goldstone [16]. This large n behavior describes tunneling through a barrier of size $n^\alpha \times n^\beta$ in the setting of n symmetric qubits. The folklore result is restricted as it only works for $\alpha < \beta$ and $\alpha < 1/2$, and it predicts constant, polynomial, or exponential scaling of the minimum gap g_{\min} depending on the barrier size. The proof of this result has not been formally published.

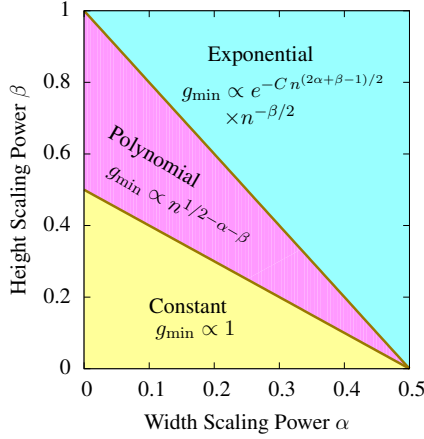


FIG. 2: The spectral gap scaling during QAO tunneling through a barrier of size $n^\alpha \times n^\beta$. Unlike Fig. 1, this figure displays all current knowledge of each region, which includes the case $\alpha > \beta$. The yellow “Constant” region was proven by Reichardt [3], and the blue “Exponential” region was shown in [14, 15] up to the polynomial prefactor. The current article proves the polynomial scaling $g_{\min} \propto n^{1/2-\alpha-\beta}$ for the red region with $1/2 < \alpha + \beta$ and $2\alpha + \beta < 1$. Our article also determines the polynomial prefactor for the blue exponential region described by $1 < 2\alpha + \beta$ with $g_{\min} \propto n^{-\beta/2} \exp(-C n^{(2\alpha+\beta-1)/2})$.

$n^\alpha \times n^\beta$ barrier scales as a function of n like

$$g_{\min} \propto \begin{cases} 1 & \text{if } \alpha + \beta \leq \frac{1}{2}, \\ n^{1/2-\alpha-\beta} & \text{if } \alpha + \beta > \frac{1}{2} \text{ and } 2\alpha + \beta \leq 1, \\ p(n) \exp(-C n^{(2\alpha+\beta-1)/2}) & \text{if } 2\alpha + \beta > 1, \end{cases} \quad (9)$$

where $p(n)$ is some polynomial in n .

While this result has never been published, its derivation is

known to use “large spin and instanton methods” [16]. Fig. 1 shows the scaling behavior according to [16]. Parts of Goldstone’s result have been verified by several other sources.

Reichardt [3] rigorously proved the existence of the constant region, and his results apply to the entire region where $\alpha + \beta < 1/2$ not just for $\alpha < \beta$. Recently, Kong and Crosson [15] verified the behavior of the gap in the exponential region for $2\alpha + \beta > 1$ using the instanton method [17], and Jiang et al. [14] have also found the same exponential scaling behavior for the runtime of thermally assisted quantum annealing on this barrier problem using a WKB approach. In a previous article [11] we numerically analyzed the transition between the polynomial and exponential regions. Notably, no previously published work has been able to verify the polynomial region, and while Kong and Crosson [15] proved the exponential region scaling, they restricted their proof to $\alpha < \beta$ and did not derive the polynomial prefactor. The different scaling regions in α and β are shown in Fig. 2, with references in the figure caption to which sources proved that region’s scaling behavior, including what is proven in this paper.

The goal of the current article is to explore both the polynomial region between $\alpha + \beta > 1/2$ and $2\alpha + \beta < 1$ and in general the region where $\alpha > \beta$. We develop elementary techniques to analyze the spectral gap and verify the polynomial, $n^{1/2-\alpha-\beta}$, scaling behavior, and we show that the results of Eq. 9 are valid even when $\alpha > \beta$.

IV. LARGE SPIN APPROXIMATION

Our Hamiltonian readily lends itself to reinterpretation as the Hamiltonian for a single particle with spin $J = n/2$. A common analytic technique for dealing with a spin Hamiltonian is to use spin coherent states [18] to create a semiclassical continuous version of the Hamiltonian. Several groups [2, 15] have used spin coherent states to analyze qubit systems, and Kong and Crosson [15] have employed spin coherent states to analyze the symmetric barrier problem for exponentially small gaps. We use a similar technique employing a modified and formalized version of the Villain transformation [19]. The Villain transformation has been used for similar problems [21–23]; in this article, we present a more formal approach to this transformation in Appendix A.

If we re-imagine our Hilbert space as representing a spin $J = n/2$ particle and associate \hat{J}_z eigenstates $|m\rangle$ with $|h\rangle$ states through $|m\rangle = |h - J\rangle$, then our symmetric Hamiltonian can be rewritten in terms of spin operators \hat{J}_i as

$$\hat{H}(s) = -(1-s)\hat{J}_x + s\hat{J}_z + s b(\hat{J}_z + J) + J\Delta, \quad (10)$$

where Δ represents some constant. Since we only care about energy differences, this constant Δ can be arbitrary, and later, we use it to ensure that the bottom of our potential energy well sits at zero energy.

Large spin techniques then pull a factor of $J = n/2 =: 1/\varepsilon$ out of our Hamiltonian so that we are dealing with operators $\hat{j}_i = \varepsilon \hat{J}_i$ that have eigenvalues that run from -1 to $+1$. Specifically, we call the \hat{j}_z eigenvalue $-1 \leq q \leq 1$, and in the

large J (i.e. small ε) limit, q can be treated as a continuous variable. We also introduce $r(q) := \varepsilon b(Jq + J)$ that is zero everywhere except in the vicinity of $q = -1/2$ where there is a bump of width $\varepsilon^{1-\alpha}$ and height $\varepsilon^{1-\beta}$. Our Hamiltonian can be rewritten as

$$\varepsilon \hat{H}(s) = -(1-s)\hat{j}_x + s\hat{j}_z + sr(\hat{j}_z) + \Delta. \quad (11)$$

At this point, we can write an approximate Schrödinger equation for this Hamiltonian using the Villain transformation. In Appendix A, we have taken the standard Villain transformation and made its logic more formal, applying it specifically to Eq. 11. In making the logic more formal, we have held off taking the continuum limit of q as long as possible. The end result of the Villain transformation itself before making any assumptions about the properties of our eigenstates gives a continuum Schrödinger equation:

$$\begin{aligned} \varepsilon E \psi(q) = & \left(sq + sr(q) + \Delta - (1-s)\sqrt{1-q^2} \right. \\ & \left. - (1-s)\frac{\varepsilon^2}{2}\sqrt{1-q^2}\frac{\partial^2}{\partial q^2} + \mathcal{O}(\varepsilon) \right) \psi(q). \end{aligned} \quad (12)$$

The first line includes a potential energy, and the next one contains the kinetic term for the problem. Note that the norm of the second derivative operator, $\frac{\partial^2}{\partial q^2}$, is proportional to ε^{-2} which is why this term survives. At this point, the problem cannot be simplified without making reference to the eigenstates we want to solve for. Notably, if we assume we are at $s^* = \frac{1}{2}(\sqrt{3}-1)$ where the minimum of the potential energy is at $q = -\frac{1}{2}$ in the $\varepsilon \rightarrow 0$ limit and make reasonable assumptions about the nature of the ground state and first excited state, then Eq. 12 can be simplified even more. In Appendix A, we formalize these approximations, and in Sec. V we analyze the resulting approximate differential equation.

V. QUADRATIC POTENTIAL APPROXIMATION

In Appendix A, we continue our approximation of Eq. 12 by noting that the low-lying energy states for $s^* = \frac{1}{2}(\sqrt{3}-1)$ are centered in the extremely close vicinity of $q = -1/2$. This allows us to focus on the variable $x := q + \frac{1}{2}$ and the region near $x = 0$. For the low-lying energy states, such as the ground state and first-excited state that we care about, the approximate differential equation representing our problem in the small ε limit is

$$\frac{\partial^2 \psi}{\partial x^2} = \frac{1}{\varepsilon^2} \left[\omega^2 x^2 + \frac{4}{3}r(x - \frac{1}{2}) - c\varepsilon E \right] \psi(x), \quad (13)$$

where $c := 8/(3(\sqrt{3}-1))$ and $\omega := 4/3$.

The potential has become an ordinary quadratic well, so we can use standard techniques from the quantum harmonic oscillator to solve the Schrödinger equation. Furthermore, since the width of the barrier $r(x-1/2)$ is proportional to $\varepsilon^{1-\alpha}$ and the height is proportional to $\varepsilon^{1-\beta}$, in the region of the barrier,

it will overshadow the quadratic potential in the small ε limit if $(\varepsilon^{1-\alpha})^2 < \varepsilon^{1-\beta}$ which translates to $1 > 2\alpha - \beta$. If we restrict ourselves to $\alpha < 1/2$ and $\beta > 0$, this is always true, so we can treat the barrier as the dominant factor in the region where $|x| = \mathcal{O}(\varepsilon^{1-\alpha})$. Therefore, we can say that the following is a good approximation for our problem in the large n limit:

$$\frac{\partial^2 \psi}{\partial x^2} = \varepsilon^{-2} [V(x) - \varepsilon c E] \psi(x) \quad (14)$$

where

$$V(x) = \begin{cases} \varepsilon^{1-\beta} & \text{if } -a < x < a \\ \omega^2 x^2 & \text{otherwise} \end{cases}, \quad (15)$$

where $a := \frac{1}{2}\varepsilon^{1-\alpha}$. In Eq. 15 we have settled on a form of $r(q)$ that is just a step function. We have focused on the step function barrier since it makes the differential equation in Eq. 14 easy to solve, but we have done numerics that indicate other barrier shapes, such as binomial or Gaussian barriers, give similar scaling results for g_{\min} .

VI. ASYMPTOTIC EXPANSION

In this section, we focus on the differential equation in Eq. 14 and find the spectral gap. Since Eq. 14 describes our original n dimensional hypercube problem in the large n limit, an asymptotic analysis of Eq. 14 in the small ε limit will give us the correct asymptotics for the original problem.

Outside of the barrier, the Schrödinger equation looks like that of an ordinary quantum harmonic oscillator problem, but we cannot use the standard harmonic oscillator solutions since these have already had boundary conditions imposed, ensuring that the wave-functions go to zero as $x \rightarrow \pm\infty$. To get the solutions for arbitrary boundary conditions, we can compare the harmonic oscillator equation to the Weber equation [24]

$$\frac{d^2 D_\nu(z)}{dz^2} + \left(\nu + \frac{1}{2} - \frac{1}{4}z^2 \right) D_\nu(z) = 0, \quad (16)$$

where ν is an arbitrary eigenvalue, and $D_\nu(z)$ is known as a parabolic cylinder function. Note that when ν is a positive integer and z is real, these functions become the standard Gaussians times Hermite polynomials we expect from the harmonic oscillator.

When ν is not a positive integer and z is real, these functions blow up as $z \rightarrow -\infty$ but go to zero as $z \rightarrow \infty$, so we can use these as the solution to our DE for $x > a$. Furthermore, to get the solution in the $x < -a$ region, we can just employ the symmetry of our problem about $x = 0$ to say that we either have symmetric or anti-symmetric eigenfunctions. Therefore, the eigen-solutions to our differential equation will have the form

$$\psi(x) = \begin{cases} \pm A_1 D_{\nu_\pm} \left(-\sqrt{\frac{2\omega}{\varepsilon}} x \right) & \text{if } x < -a \\ A_2 e^{k_\pm x} \pm A_2 e^{-k_\pm x} & \text{if } -a < x < a, \\ A_1 D_{\nu_\pm} \left(\sqrt{\frac{2\omega}{\varepsilon}} x \right) & \text{if } x > a \end{cases} \quad (17)$$

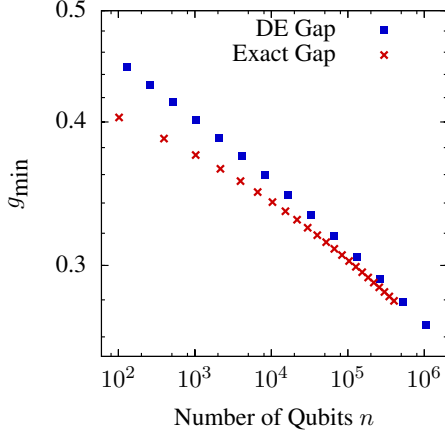


FIG. 3: Comparison between the scaling of the true spectral gap obtained by diagonalization of Eq. 7 and the gap obtained by solving for the eigenenergies of the differential equation in Eq. 14. The latter is calculated by numerically solving the transcendental equation in Eq. 18. Note that these scalings converge for $n > 10^5$, confirming that our derivation of Eq. 14 is indeed valid in the limit of large n . This data was obtained for a rectangular barrier with $\alpha = \beta = 0.3$.

where $\nu_{\pm} := \frac{cE_{\pm}}{2\omega} - \frac{1}{2}$ and $k_{\pm} := \sqrt{\varepsilon^{-1-\beta} - \varepsilon^{-1}cE_{\pm}}$.

By applying continuity in the wave-function and its derivative across the boundary at $x = \pm a$, we can find a transcendental equation for the energies, which we denote by E_{\pm} representing the two lowest level energy states:

$$k_{\pm} D_{\nu_{\pm}} \left(\sqrt{\frac{2\omega}{\varepsilon}} a \right) (e^{k_{\pm} a} \mp e^{-k_{\pm} a}) = \sqrt{\frac{2\omega}{\varepsilon}} D'_{\nu_{\pm}} \left(\sqrt{\frac{2\omega}{\varepsilon}} a \right) (e^{k_{\pm} a} \pm e^{-k_{\pm} a}). \quad (18)$$

This transcendental equation can be solved numerically for the lowest energy levels, and a comparison of this numerical solution to the full spectral gap of the Hamiltonian in Eq. 7 is shown in Fig. 3. In the rest of this section, we show that we can do better than numerical solutions to Eq. 18 by finding an asymptotic solution in the limit of large n .

We expect the energies to be close to the unperturbed first excited state energy of $E_1 = 3\omega/c$, so we say $E_{\pm} = (3\omega + \delta_{\pm})/c$ and find δ_{\pm} in the limit of small ε . In this limit $\nu_{\pm} = \frac{\delta_{\pm}}{2\omega} + 1$ and $k_{\pm} \approx \varepsilon^{-\frac{1}{2}-\frac{\beta}{2}}$.

At this point, we want to calculate $g_{\min} = |\delta_+ - \delta_-|/c$ up to leading order in ε using these approximations. If we assume that $2\alpha + \beta < 1$, $\alpha < 1/2$, and $\alpha + \beta > 1/2$ (this corresponds to the polynomial region in Fig. 2), then the gap becomes

$$g_{\min} = \frac{8(\omega)^{3/2}}{c\sqrt{\pi}} \varepsilon^{\alpha+\beta-\frac{1}{2}} \propto n^{\frac{1}{2}-\alpha-\beta}. \quad (19)$$

Similarly, if we assume $2\alpha + \beta > 1$ and $\alpha < 1/2$, then the

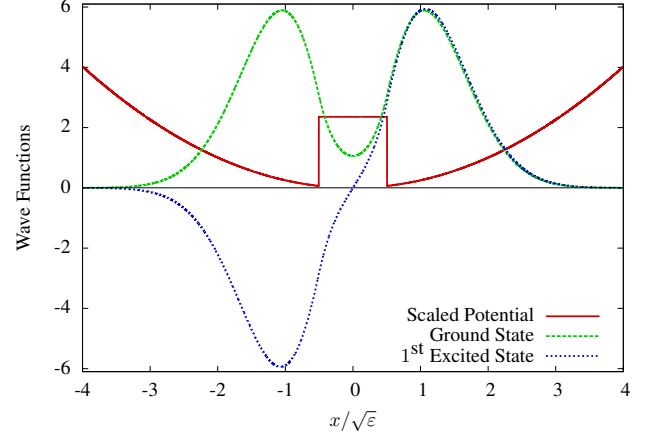


FIG. 4: The ground state and first excited state wave functions for the quadratic well approximation of Eq. 14. We also display the potential energy from Eq. 15 multiplied by a factor of $10/\sqrt{\varepsilon}$ so that it is fully visible. Notice that the ground state looks like a Gaussian with the middle dragged downward and the first excited state looks unchanged from the unperturbed quantum harmonic oscillator since the barrier sits in a region where this function was already small.

gap becomes

$$g_{\min} = \frac{16(\omega)^{3/2}}{c\sqrt{\pi}} \varepsilon^{\beta/2} \exp\left(-\varepsilon^{\frac{1}{2}-\alpha-\frac{\beta}{2}}\right) \propto n^{-\frac{\beta}{2}} \exp\left(-(n/2)^{\alpha+\frac{\beta}{2}-\frac{1}{2}}\right). \quad (20)$$

This result matches the exponentially small gap found by Kong and Crosson [15] and Jiang et al. [14].

The dependences on ε in Eqs. 19 and 20 are exactly what we would expect given Eq. 9. Notice that we do not need to assume $\alpha < \beta$ as in Eq. 9, so our result extends farther than Goldstone's result and covers the entire area bounded by $0 < \alpha < 1/2$ and $\alpha + \beta > 1/2$.

In Fig. 4, we plot the exact ground state and first excited state for the quadratic approximation for $\varepsilon = 1/5000$, a bump width of $1/70$, and a bump height of $1/300$. These values were chosen to provide visibility for the bump and its effect on the eigenfunctions. The potential is also plotted, multiplied by $10/\sqrt{\varepsilon}$ so that it is visible. Here we are using the exact energies, obtained by solving the transcendental equation, Eq. 18, numerically. Notice that the ground state looks like a Gaussian with its center pulled down whereas the first excited state looks almost unchanged from its unperturbed state. The first excited state is unchanged because it was already small in the vicinity of $x = 0$, so the barrier does not alter this state much by making that region more unfavorable. This is also reflected in our approximation in Eq. 19 where the leading order term shown here is due to the ground state rather than the first excited state.

VII. CONCLUSION

We have taken our original n qubit barrier tunneling problem and, through a series of large- n approximations, have arrived at an elementary barrier tunneling problem in one continuous dimension. The resulting approximate Schrödinger equation gives a transcendental equation for the energies that in the large- n limit gives a spectral gap that is proportional to $1/n^{\alpha+\beta-\frac{1}{2}}$ for $1/2 < \alpha + \beta$ and $2\alpha + \beta < 1$, and $n^{-\beta/2} \exp(-Cn^{(2\alpha+\beta-1)/2})$ when $1 < 2\alpha + \beta$. Our gap scaling result verifies and provides a solid proof the 2002 folklore result by Goldstone [16].

Combined with the work of Reichardt [3] and Kong and Crosson [15], our result provides a full picture of the asymp-

totic behavior of the spectral gap during barrier tunneling for a symmetric cost function on n qubits. Additionally, our method holds no matter where the barrier is centered (with suitable redefinitions of some of the constants involved). Our work does focus on a step function barrier and can therefore be made more general in terms of barrier shape, but numerics indicate that other barrier shapes give the same scaling for g_{\min} .

Acknowledgements

This material is based upon work supported by the National Science Foundation under Grant No. 1314969.

-
- [1] E. Farhi, J. Goldstone, S. Gutmann, M. Sipser, quant-ph/0001106 (2000)
 - [2] E. Farhi, J. Goldstone, S. Gutmann, quant-ph/0201031 (2002)
 - [3] B. W. Reichardt, in Proceedings of the 36th Annual ACM Symposium on Theory of Computing (STOC'04), ACM Press(2004)
 - [4] E. Farhi, J. Goldstone, S. Gutmann, D. Nagaj. Int. J. Quantum Inf. **6**, 3 (2008)
 - [5] R. Martoňák, G. E. Santoro, E. Tosatti. Phys. Rev. B **66**, 094203 (2002)
 - [6] M. B. Hastings, M. H. Freedman. Quant. Inf. & Comp. **13**, 11-12 (2013)
 - [7] S. Boixo, T. F. Rønnow, S. V. Isakov, Z. Wang, D. Wecker, D. A. Lidar, J. M. Martinis, M. Troyer, Nature Phys. **10**, 218 (2014)
 - [8] E. Crosson, M. Deng, quant-ph/1410.8484 (2014)
 - [9] B. Heim, T. F. Rønnow, S. V. Isakov, M. Troyer, Science **348**, 6231 (2015)
 - [10] S. Muthukrishnan, T. Albash, D. A. Lidar, quant-ph/1505.01249 (2015)
 - [11] L. Brady, W. van Dam, quant-ph/1509.02562 (2015)
 - [12] S. V. Isakov, G. Mazzola, V. N. Smelyanskiy, Z. Jiang, S. Boixo, H. Neven, M. Troyer quant-ph/1510.08057 (2015)
 - [13] E. Crosson, A. W. Harrow, quant-ph/1601.03030 (2016)
 - [14] Z. Jiang, V. N. Smelyanskiy, S. V. Isakov, S. Boixo, G. Mazzola, M. Troyer, H. Neven, quant-ph/1603.01293 (2016)
 - [15] L. Kong, E. Crosson, quant-ph/1511.06991 (2015)
 - [16] J. Goldstone (unpublished), 2002.
 - [17] S. Coleman. *Aspects of Symmetry*. Cambridge University Press, 1985.
 - [18] A. Auerbach. *Interacting Electrons and Quantum Magnetism*. Springer-Verlag, 1994.
 - [19] J. Villain, J. Physique, **35**, 27 (1974).
 - [20] S. Jansen, M. Ruskai, R. Seiler, J. Math. Phys. **48**, 102111 (2007)
 - [21] M.ENZ, R. Schilling, J. Phys. C: Solid State Phys. **19** (1986).
 - [22] A. Boulatov, V. N. Smelyanskiy, Phys. Rev. A **68**, 062321 (2003).
 - [23] S. Boixo et al. arXiv:1411.4036 (2014)
 - [24] E. Weisstein, "Parabolic Cylinder Function." MathWorld—A Wolfram Web Resource.

Appendix A: Discrete Villain Transformation

Our goal in this appendix is to fill in the gaps in the derivation of Eq. 13, starting from Eq. 11. The Villain representation [19] is a standard semi-classical approximation which first takes the continuum limit of the eigenvalues of \hat{j}_z and then defines a conjugate momentum to this continuous "position" variable. This technique, as it is commonly implemented, has many subtleties that are ignored, so this appendix formalizes the assumptions implicit in the Villain representation. Furthermore, we extend these results and show that certain assumptions about the ground and first excited states allow us to refine our approximations and improve the analysis of the barrier tunneling problem. We also derive all of our results in the discrete case, only resorting to the continuum limit at the end, elucidating the nature of our assumptions.

The original Villain transformation [19] says that \hat{j}_z and $\hat{j}_{\pm} := \hat{j}_x \pm i\hat{j}_y$ act on the \hat{j}_z eigenkets with the following relations

$$\begin{aligned}\hat{j}_z|q\rangle &= q|q\rangle \\ \hat{j}_+|q\rangle &= e^{-ip}\sqrt{1+\varepsilon-q(q+\varepsilon)}|q\rangle \\ \hat{j}_-|q\rangle &= \sqrt{1+\varepsilon-q(q+\varepsilon)}e^{ip}|q\rangle\end{aligned}\quad (\text{A1})$$

Here p is the conjugate momentum for q , and in q -space it can be represented as $p = -i\varepsilon\frac{\partial}{\partial q}$. Many users [21–23] of the Villain representation employ the small ε limit to say that the square root factors in the \hat{j}_{\pm} expressions are approximately equal and that the commutators between q and p are negligible. Using these approximations, they find that

$$\hat{j}_x = \frac{1}{2}(\hat{j}_+ + \hat{j}_-) = \sqrt{1+q^2}\cos p. \quad (\text{A2})$$

These small ε approximations ignore many subtleties, most centering around how big p is. Eq. A2 is true only to zeroth order in ε , but because the derivative operator has an operator norm that is proportional to ε^{-1} , there is a relevant term to second order in p . However, this expression is incorrect at all higher orders of ε and in fact includes terms linear in p that

are not included here. One of the most misleading errors is that the true expression for \hat{j}_x contains no terms with higher order of p than p^2 .

Below, we go through a more formal derivation of \hat{j}_x 's expansion using the underlying matrices and proceed with a description of how the discrete Villain transformation can be used in the setting of the barrier tunneling problem.

1. Discrete j -operators

We remind the reader that $\varepsilon = 2/n = 1/J$, and we start by examining \hat{j}_x in the eigenbasis of \hat{j}_z given by $|q\rangle$ where $q = \varepsilon m \in [-1, +1]$ for $m \in \{-J, -J+1, \dots, J\}$. Our goal will be to determine how \hat{j}_x acts on a general state $|\psi\rangle$:

$$\hat{j}_x|\psi\rangle = \sum_q \hat{j}_x \psi_q |q\rangle \quad (\text{A3})$$

We introduce three new operators which will simplify the representation of the raising and lowering operators \hat{j}_\pm :

$$\hat{P} = \sum_{q \in [-1, 1-\varepsilon]} |q+\varepsilon\rangle\langle q| \quad \text{and} \quad \hat{M} = \sum_{q \in [-1+\varepsilon, 1]} |q-\varepsilon\rangle\langle q| \quad (\text{A4})$$

$$\hat{q} = \sum_q q |q\rangle\langle q|.$$

Since \hat{q} is diagonal, functions of the operator are diagonal themselves, and the first two operators extract just raising and lowering of indices without any prefactors. Therefore, we can represent \hat{j}_x as

$$\begin{aligned} \hat{j}_x &= \frac{1}{2}(\hat{j}_+ + \hat{j}_-) \\ &= \frac{1}{2} \left(\sqrt{(1-\hat{q})(1+\hat{q}+\varepsilon)} \hat{P} + \sqrt{(1+\hat{q})(1-\hat{q}+\varepsilon)} \hat{M} \right). \end{aligned} \quad (\text{A5})$$

Our eventual goal is to take a continuum limit of q and then represent \hat{j}_x in terms of the continuous q and its derivatives. We can create a dictionary for the matrices that lead to derivatives in the limit that $\langle q|\psi\rangle = \psi_q \rightarrow \psi(q)$:

$$\begin{aligned} \frac{\partial \psi}{\partial q} &= \lim_{\varepsilon \rightarrow 0} \frac{\psi(q+\varepsilon) - \psi(q-\varepsilon)}{2\varepsilon} \\ &= \lim_{\varepsilon \rightarrow 0} \frac{\psi_{q+\varepsilon} - \psi_{q-\varepsilon}}{2\varepsilon} = \lim_{\varepsilon \rightarrow 0} (\hat{A}\vec{\psi})_q, \end{aligned} \quad (\text{A6})$$

$$\begin{aligned} \frac{\partial^2 \psi}{\partial q^2} &= \lim_{\varepsilon \rightarrow 0} \frac{\psi(q+\varepsilon) - 2\psi(q) + \psi(q-\varepsilon)}{\varepsilon^2} \\ &= \lim_{\varepsilon \rightarrow 0} \frac{\psi_{q+\varepsilon} - 2\psi_q + \psi_{q-\varepsilon}}{\varepsilon^2} = \lim_{\varepsilon \rightarrow 0} (\hat{B}\vec{\psi})_q. \end{aligned} \quad (\text{A7})$$

Here we have defined two new operators that correspond to the discrete versions of our first and second derivatives:

$$\varepsilon \hat{A} = \frac{\hat{P} - \hat{M}}{2} \quad \text{and} \quad \varepsilon^2 \hat{B} = \hat{P} - 2\hat{I} + \hat{M}. \quad (\text{A8})$$

Throughout this appendix, we refer to the relative sizes of operators using their matrix norm. The definition of the matrix norm we are using is the maximum absolute value of any eigenvalue of the operator. Therefore, the norm of \hat{A} is proportional to ε^{-1} , and the norm of \hat{B} is proportional to ε^{-2} . We come back to revisit this concept later in the context of our specific eigenstates.

Based on the definitions in Eq. A8, we can rewrite \hat{P} and \hat{M} in terms of \hat{I} , \hat{A} , and \hat{B} :

$$\hat{P} = \hat{I} + \varepsilon \hat{A} + \frac{\varepsilon^2}{2} \hat{B} \quad \text{and} \quad \hat{M} = \hat{I} - \varepsilon \hat{A} + \frac{\varepsilon^2}{2} \hat{B}. \quad (\text{A9})$$

Notice that in the continuous form of the Villain representation, Eq. A1, the operators, \hat{P} and \hat{M} , correspond to $e^{\mp i p}$, but in Eq. A9 we see that the operators only correspond to the first two terms in the Taylor expansion of the exponentials. In addition, the matrix norms of \hat{A} and \hat{B} further complicate the issue, making it deceptively appear that the later terms in the series are smaller when in fact every term in this series is roughly equivalent in size, relative to ε .

We use the expansions in Eq. A9 with Eq. A5 to obtain a discrete form of the Villain representation. It should be noted that the following expression is exact and includes no approximations yet

$$\begin{aligned} \hat{j}_x &= \frac{1}{2} \left(\sqrt{(1-\hat{q})(1+\hat{q}+\varepsilon)} \left[\hat{I} + \varepsilon \hat{A} + \frac{\varepsilon^2}{2} \hat{B} \right] \right. \\ &\quad \left. + \sqrt{(1+\hat{q})(1-\hat{q}+\varepsilon)} \left[\hat{I} - \varepsilon \hat{A} + \frac{\varepsilon^2}{2} \hat{B} \right] \right) \end{aligned} \quad (\text{A10})$$

Next, we begin taking the large spin limit by expanding the square root prefactors in orders of ε

$$\sqrt{(1 \mp \hat{q})(1 \pm \hat{q} + \varepsilon)} = \sqrt{1 - \hat{q}^2} + \varepsilon \frac{1 \mp \hat{q}}{2\sqrt{1 - \hat{q}^2}} + \mathcal{O}(\varepsilon^2) \quad (\text{A11})$$

Combining Eq. A10 and Eq. A11 results in a discrete form of the Villain representation for \hat{j}_x :

$$\begin{aligned} \hat{j}_x &= \frac{1}{2} \left(\left[2\sqrt{1 - \hat{q}^2} + \frac{\varepsilon}{\sqrt{1 - \hat{q}^2}} \right] - \varepsilon^2 \frac{\hat{q}}{\sqrt{1 - \hat{q}^2}} \hat{A} \right. \\ &\quad \left. + \varepsilon^2 \left(\sqrt{1 - \hat{q}^2} + \frac{\varepsilon}{2\sqrt{1 - \hat{q}^2}} \right) \hat{B} + \mathcal{O}(\varepsilon^2) \right). \end{aligned} \quad (\text{A12})$$

Here we have kept terms that are at most proportional to ε , remembering that the norms of \hat{A} and \hat{B} are proportional to ε^{-1} and ε^{-2} respectively. The expression in Eq. A12 can be thought of as a more accurate version of Eq. A2, and up to zeroth order in ε , Eq. A12 and Eq. A2 agree.

Some knowledge of the specific eigenstates can restrict the form of Eq. A12 even more, allowing us to consider the maximum eigenvalue of \hat{A} and \hat{B} relevant to the low energy eigenvectors of our problem, rather than the maximum eigenvalues obtainable for a general problem.

There are a few key things to note about Eq. A12 in relation to Eq. A2. First, we only have terms up to the second derivative, even including all orders in ε . Second, this form of the operator makes no assumptions about the specific form of the Hamiltonian or its energy states. If, as we do in the next section, we make assumptions about the energy states of the barrier tunneling problem, we can further approximate the expression for \hat{j}_x into a simpler form.

2. Hamiltonian and Eigenstate-based Approximations

Eq. A12 can be used with the barrier tunneling Hamiltonian:

$$\varepsilon \hat{H} = -(1-s)\hat{j}_x + s\hat{j}_z + sr(\hat{j}_z) + \Delta \quad (\text{A13})$$

The operator \hat{j}_z is equivalent to \hat{q} , and \hat{j}_x can be replaced using Eq. A12, interpreting $\vec{\psi}$ as an eigenstate with eigenenergy E , so that the Schrödinger equation becomes

$$\begin{aligned} \varepsilon E|\psi\rangle = & \left(s\hat{q} + sr(\hat{q}) + \Delta - (1-s) \left[\sqrt{1-\hat{q}^2} + \frac{\varepsilon}{2\sqrt{1-\hat{q}^2}} \right] \right) |\psi\rangle \\ & + (1-s) \frac{\varepsilon^2}{2} \frac{\hat{q}}{\sqrt{1-\hat{q}^2}} \hat{A} \\ & - (1-s) \frac{\varepsilon^2}{2} \left(\sqrt{1-\hat{q}^2} + \frac{\varepsilon}{2\sqrt{1-\hat{q}^2}} \right) \hat{B} + \mathcal{O}(\varepsilon^2) |\psi\rangle. \end{aligned} \quad (\text{A14})$$

Eq. 12 is a continuum limit version of this equation, where q is treated as a continuous variable so that $\hat{q} \rightarrow q$, $\vec{\psi} \rightarrow \psi(q)$, $\hat{A} \rightarrow \frac{\partial \psi}{\partial q}$, and $\hat{B} \rightarrow \frac{\partial^2 \psi}{\partial q^2}$.

Next, we define the operator $\hat{x} = \hat{q} + \frac{1}{2}$ and call the diagonal entries of this operator $x = q + \frac{1}{2}$. The advantage of this variable, x , is that it is small in the vicinity of $q = -\frac{1}{2}$ where the tunneling event occurs. Since the critical tunneling moment and minimum spectral gap occur at $s^* = \frac{1}{2}(\sqrt{3}-1)$, the rest of this appendix will set $s = s^*$.

Nex, we look more closely at \hat{x} and its relationship to $|\psi\rangle$. The low energy eigenvectors, $|\psi\rangle$, are essentially zero for most of their entries except right around the location of the primary bump in the distribution. The reasoning behind this comes from the fact that for the low-lying energy states, their energy is lower than the potential energy function for the entire range of x , except in an extremely narrow range around the barrier, leading to exponential suppression of the wave functions outside this region. For the no barrier case, the ground state and first excited state both have width $\mathcal{O}(\sqrt{\varepsilon})$ and are centered around $x = 0$ with exponential suppression farther away from $x = 0$.

Since the widths of the ground state and first excited state ($\mathcal{O}(\sqrt{\varepsilon})$) are larger than the width of the barrier ($\mathcal{O}(\varepsilon^{1-\alpha})$), the range of x over which the components of $|\psi\rangle$ are non-zero is $\mathcal{O}(\sqrt{\varepsilon})$. Therefore, focusing on the diagonal terms in the Schrödinger equation that do not include \hat{A} or \hat{B} , we can expand these to order ε by treating $\|\hat{x}|\psi\rangle\| \in \mathcal{O}(\sqrt{\varepsilon})$ since for

the non-zero components of $|\psi\rangle$, the typical x values will be of order $\sqrt{\varepsilon}$. We also use an arbitrary constant Δ to cancel out the constant terms in the expansion, physically ensuring that the bottom of the potential well is at zero energy:

$$\begin{aligned} & \left(s^* \hat{q} + \Delta - (1-s^*) \left[\sqrt{1-\hat{q}^2} + \frac{\varepsilon}{2\sqrt{1-\hat{q}^2}} \right] \right) |\psi\rangle = \\ & \left(\frac{2}{3}(\sqrt{3}-1)\hat{x}^2 \right) |\psi\rangle + \mathcal{O}(\varepsilon^{3/2}), \end{aligned} \quad (\text{A15})$$

where $\Delta = -\frac{(\sqrt{3}-1)}{24}(24+12\varepsilon)$.

Next, we focus on the derivative terms of Eq. A14 that include \hat{A} and \hat{B} . We expect the size of the derivative to be governed by the inverse of the length scale over which the eigenvector components change. In the unperturbed case, we expect the eigenvector (which is a binomial distribution) components to change on a length scale of $\sqrt{\varepsilon}$ which would mean that \hat{A} scales like $1/\sqrt{\varepsilon}$ and \hat{B} scales like $1/\varepsilon$. Note that these would then correspond to the norms $\|\hat{A}|\psi\rangle\|$ and $\|\hat{B}|\psi\rangle\|$ not $\|\hat{A}\|$ and $\|\hat{B}\|$ which as we discussed in the last section can be much larger. This scaling behavior requires our restriction to the low-lying energy states.

In the perturbed case, we expect the shortest length scale in the problem to be governed by the exponential decay inside the barrier. In the prototypical barrier tunneling problem of plane waves tunneling through a square barrier, the Schrödinger equation inside the barrier, which will have extent $-\xi < y < \xi$, will be of the form

$$\frac{d^2 \varphi}{dy^2} = \frac{2}{\hbar^2} (V_0 - \mathcal{E}) \varphi(y) = k^2 \varphi(y). \quad (\text{A16})$$

The simple Schrödinger equation in Eq. A16 can be transformed into our problem by taking $\hbar \rightarrow \varepsilon$, setting the width of the barrier ξ to be proportional to $\varepsilon^{1-\alpha}$, setting the height of the barrier, V_0 , to be proportional to $\varepsilon^{1-\beta}$, and making the energy, \mathcal{E} , much smaller than V_0 in the small ε limit. If we compare this to our expression in Eq. A14, we see that at the very least there is still a factor of ε^2 in the ratio between the potential barrier $r(q)$ and the second derivative term \hat{B} . This is a rough comparison, but we can use it to inform what the exponential decay inside the barrier looks like.

Specifically, Eq. A16 is solved by $e^{\pm k y}$, where in our case k is proportional to $\varepsilon^{-\frac{1}{2}-\frac{\beta}{2}}$, assuming that $V_0 \gg \mathcal{E}$, which is a good assumption in our problem. Therefore, the length scale over which the wavefunction changes inside the barrier is proportional to $\varepsilon^{\frac{1}{2}+\frac{\beta}{2}}$. This means that we can claim our derivative, and therefore \hat{A} , scales like $\varepsilon^{-\frac{1}{2}-\frac{\beta}{2}}$, and similarly \hat{B} scales like $\varepsilon^{-1-\beta}$. Alternatively, the derivatives are proportional to k and k^2 for \hat{A} and \hat{B} respectively.

One other thing to note is that if we are looking at a derivative that scales like $\varepsilon^{\frac{1}{2}+\frac{\beta}{2}}$, it will only have this extreme scaling in the region close to the edge of the barrier, which means that $x \in \mathcal{O}(\varepsilon^{1-\alpha})$ when we care about derivatives that are this large. Thus in keeping track of the order, we need to remember that higher order terms in x will be even more exacerbated in this region of the barrier.

The next two equations focus on just the lowest order terms that include \hat{A} and \hat{B} . Using the approximations stated in the last few paragraphs, the lowest order term containing \hat{A} becomes

$$(1 - s^*)\varepsilon^2 \frac{\hat{q}}{2\sqrt{1 - \hat{q}^2}} \hat{A} = -\frac{1}{2}(\sqrt{3} - 1)\varepsilon^2 \hat{A} + \mathcal{O}(\varepsilon^{\frac{5}{2} - \alpha - \frac{\beta}{2}}) = \mathcal{O}(\varepsilon^{\frac{3}{2} - \frac{\beta}{2}}), \quad (\text{A17})$$

while for \hat{B} the term becomes

$$-(1 - s^*)\frac{\varepsilon^2}{2} \left(\sqrt{1 - \hat{q}^2} + \frac{\varepsilon}{2\sqrt{1 - \hat{q}^2}} \right) \hat{B} = -\frac{3}{8}(\sqrt{3} - 1)\varepsilon^2 \hat{B} + \mathcal{O}(\varepsilon^{2 - \alpha - \beta}) = \mathcal{O}(\varepsilon^{1 - \beta}) \quad (\text{A18})$$

Our condition for whether a term is discounted as too small or not depends on whether it is larger than the energy term. Our unperturbed energies are constant with ε , but notice that E is multiplied by ε in the Schrödinger equation. Thus, we expect this energy term to be proportional to ε with some polynomially or exponentially small corrections. Therefore, if a term is higher order than linear in ε , we discard it since it is smaller than the energy term which is what we care about.

We assume $\beta < 1$, in which case, the \hat{A} terms are all small. For the \hat{B} terms, we see that we need $1 < 2 - \alpha - \beta$ in order for the next highest term to contribute, so we need to restrict ourselves to $\alpha + \beta < 1$. The only remaining thing to consider

is how much the $r(\hat{q})$ term will contribute. The height of the barrier scales like $\varepsilon^{1 - \beta}$ in this setup, so as long as $\beta > 0$, the barrier term remains relevant as well. With all of these approximations, the Schrödinger equation becomes

$$\varepsilon E \vec{\psi} = \left(s^* r \left(\hat{x} - \frac{1}{2} \right) + \frac{2}{3}(\sqrt{3} - 1)\hat{x}^2 - \frac{3}{8}(\sqrt{3} - 1)\varepsilon^2 \hat{B} + \mathcal{O}(\max\{\varepsilon^{2 - \alpha - \beta}, \varepsilon^{\frac{3}{2} - \frac{\beta}{2}}\}) \right) \vec{\psi} \quad (\text{A19})$$

Eq. A19 is the final form of our approximated Schrödinger equation in the discrete setting. The continuum limit allows us to treat this as a differential equation which can be solved exactly, so the final step is to take the continuum limit. This limit takes x to a continuous variable in the small ε limit, taking $\hat{B} \rightarrow \frac{\partial^2}{\partial x^2}$, $\hat{x} \rightarrow x$, and $|\psi\rangle \rightarrow \psi(x)$. Doing this gives the differential equation

$$\varepsilon E \psi(x) = \left(s^* r \left(x - \frac{1}{2} \right) + \frac{2}{3}(\sqrt{3} - 1)x^2 - \frac{3}{8}(\sqrt{3} - 1)\varepsilon^2 \frac{\partial^2}{\partial x^2} + \mathcal{O}(\max\{\varepsilon^{2 - \alpha - \beta}, \varepsilon^{\frac{3}{2} - \frac{\beta}{2}}\}) \right) \psi(x) \quad (\text{A20})$$

This can be solved using the parabolic cylinder equations as shown in in the main text of the paper.